A Multi-Point Electrical Resistance Measurement System for Characterization of Foam Drainage Regime and Stability

Chanhyuk Park
Dept. of Civil and Environmental Engineering, University of California at Berkeley, Berkeley, CA 94720

Center for Water Resource Cycle Research, Korea Institute of Science and Technology, Seoul 136-791,
South Korea

Slawomir W. Hermanowicz
Dept. of Civil and Environmental Engineering, University of California at Berkeley, Berkeley, CA 94720

DOI 10.1002/aic.14489

Foam drainage regimes are significantly associated with the nature of the hydrodynamic resistance in foam structure. A multi-point electrical resistance measurement technique has been applied for characterization of the drainage regimes and quantifying stability within standing foams. The capacity of the technique was confirmed by the estimation of macroscopic drainage rates for aqueous foams stabilized with sodium dodecyl sulfate. The drainage of sodium dodecylbenzenesulfonate, a commercial form of linear alkylbenzene sulfonate that is the most frequently used in household detergents was studied in detail by two complementary methods (forced and free drainage). The experimental data could be fitted using a power-law with an exponent of 1/3 for forced drainage and of 1.0 for free drainage. These data indicate the following drainage behavior: mobile bubble surfaces, causing plug-like flow within Plateau borders, thus dissipation mainly occurs inside the nodes. This research introduced an accurate method for quantifying foam stability that can be assessed by variations of real-time measured foam heights that incorporate the evolution of the liquid content.

Keywords: drainage regime, electrical resistance, forced drainage, stability, sodium dodecylbenzenesulfonate

Introduction

Aqueous foam is basically a large volume of a gas, enveloped by a much smaller amount of a liquid in the presence of surfactant molecules stabilizing the gas-liquid interfaces. In various applications, foams could be produced by physical methods such as shaking, pouring, or sparging gas, or could be generated by chemical methods including fermentation, (electro-) chemical reaction, or ultrasound.[1–3] When freshly formed, foams are thermodynamically unstable and sometimes dissipate within a few seconds.[4,5] In other cases, some foam systems persist for a long time, for instance, the presence of a substantial stable layer in a bioreactor could lead to serious deleterious effects.[6–9] One of the main characteristics of foams is that they irreversibly evolve in time because they are not in equilibrium under normal gravity conditions.[10,11] Liquid drains out of the foam until such an equilibrium is attained, and some liquid is kept inside the foam due to capillary forces.[12] Liquid drainage is a complex physicochemical hydrodynamic process at the gas-liquid interfaces.[13,14] The main hydrodynamic energy-dissipation through the foam is due to the liquid flowing in the network of the channels known as Plateau borders (PBs) interconnected at the nodes.[15,16] These elementary structures (PBs and nodes) within the foam strongly depend on the liquid content, which is directly coupled to foam permeability.[13,17–19] When the liquid drains, the foam structure becomes thinner and more fragile, leading foam collapse.[20,21] Fast drainage rates are expected to indicate less stable foams, leading to a quick breakdown of foam structure. Such changes in the liquid content and the drainage rates are important for predicting foam stability.

The main objective of drainage studies was to find out how long it takes for the foam to achieve a steady state. Several methods have been extensively used to characterize liquid distribution within the foam.[15,22–24] Measuring the drainage of a standing foam (free drainage) is conceptually the simplest. The drainage rates and regimes could be determined as a decrease of the local liquid fraction at a given location.[25–27] Recent studies focused on a method with gravity-driven liquid flow with continuous supply of liquid called forced drainage. Numerous researchers carried out forced drainage experiments to investigate the drainage properties of the foam.[28–30] In such experiments, the surfactant solution is added to the top of initially dried and drained foam at a controlled flow rate, causing propagation of a continuous wet traveling wave throughout the foam height. A front of the wave is detected, separating the initially dried foam below from the wetter foam above. The wave front moves down with a constant drainage velocity, thus forming

---

Correspondence concerning this article should be addressed to C. Park at chpark@kist.re.kr.

a solitary wave. The drainage regime is determined by relating the front drainage velocity to the superficial velocity. It has been proposed that a power-law exponent of this relation is a relevant parameter that characterizes the drainage regimes (channel- or node-dominated).[13,14,20]

There are few techniques available for the study of foam drainage.[31] Foam optical properties strongly depend on the liquid content, and used in the liquid drainage based on the measurements of the transmitted light, recorded by a CCD digital camera.[18,25,32] This light transmission technique is possible to determine liquid fraction gradients and front drainage velocity, but it remains difficult to use it regarding the quantitative estimation of liquid fraction, as the details of light transport in foams are not yet well understood.[16,29] Foam electrical properties are also used to study the drainage of foams. Early measurements of foam drainage involved a segmented capacitance resistor which requires the foam to be non-conducting,[33] but the difficulties associated with calibration and the lack of reproducibility represent drawbacks for this method.[31] An improved method extensively used electrodes, which consisted of two parallel plates or two stripped wires, and measured the local electrical resistance in electrically conducting foams.[34–39] Recent technique has been developed and tested for a multi-point foam probe, which allows measurement of the electrical current across a foam phase at multiple locations.[40–42] The change in electrical current is important for the continuous monitoring of the rate of foam formation and collapse.[43] Such techniques are particularly valuable in processes where foams cannot easily be visualized, for example, foam formation in bioreactors.[38,40] However, a protocol for the electrical resistance technique to determine the appropriate drainage properties in various aqueous foams has been limited.

This study focused on the development of a systematic methodology for the characterization of foam drainage rate, regime and stability by the multi-point electrical resistance measurement technique. As compared to existing drainage studies by other measurement techniques in the literature, our methodology developed in this study was validated by correlations between the drainage velocity and the superficial velocity in the sodium dodecyl sulfate (SDS) foam column of large diameter (15.2 cm). We carried out both forced and free drainage experiments to show the drainage properties of aqueous foams stabilized with sodium dodecylbenzenesulfonate (SDBS), a commercial form of linear alkylbenzene sulfonate that comprises the majority of anionic surfactants currently manufactured by the chemical industry[44] and is the most frequently used in household detergents.[45] We finally described a half-life time of the foam estimated by the electrical resistance measurement technique, which can be used subsequently for advanced monitoring of foam development and evolution. This approach was proposed as a powerful tool for studying drainage of foams and offered practical techniques over other techniques (e.g., optical or light transmission) because it was simple, require less specialized equipment, and had minimal impact on subsequent analysis.

Drainage Model and Boundary Conditions

A theoretical model of foam drainage focuses on gravity-driven flow through aqueous foams and describes the time and space evolution of the foam liquid fraction, $\varepsilon\ (z,\ t)$.[16,18] This model is based on the local description of the liquid flow in a single foam structure (a PB and a node). The drainage equation is derived by averaging over the whole network of PBs and nodes. The foam is considered as a porous medium, but its permeability is not constant and is dynamically coupled to the liquid flow, unlike conventional porous media. Hence, the Darcy's law that relates the permeability (k) and the average front drainage velocity (v_{f}) through the foam is shown in Eq. 1 with permeability as an explicit function of $\varepsilon\ (z,\ t)$

$$v_{\mathrm{f}} = \frac{k(\varepsilon)}{\mu}\rho g \tag{1}$$

where μ is the bulk viscosity of foaming solutions, ρ is the liquid density, and g is the gravitational acceleration. The permeability of the porous medium (i.e., foam) to liquid flow is determined by the physicochemical properties of foaming solutions. A detailed derivation of a general expression for $k(\varepsilon)$ is presented in Koehler et al.[16]

In the first limiting case, assuming no-slip boundary conditions (less mobile) at the bubble surface, the liquid flowing inside the PBs is Poiseuille-like with high surface viscosity at the bubble surfaces and the permeability is $k(\varepsilon) = K_{\mathrm{c}}L^2\varepsilon$. K_{c} is the dimensionless permeability number, which depends only on the PB (channel) geometry and L is the PB length. The front velocity is given by

$$\begin{aligned} V_{\mathrm{f}} &= \frac{K_{\mathrm{c}}\rho g L^2}{\mu}\varepsilon = \left(\frac{K_{\mathrm{c}}\rho g L^2}{\mu}\right)\cdot\left(\frac{v_{\mathrm{s}}}{v_{\mathrm{f}}}\right)^{1/2} \\ &= \left(\frac{K_{\mathrm{c}}\rho g L^2}{\mu}\right)^{1/2}\cdot {v_{\mathrm{s}}}^{1/2} = \tau\cdot {v_{\mathrm{s}}}^{1/2} \end{aligned} \tag{2}$$

In the second case, assuming slip boundary conditions (mobile) at the bubble surfaces, it is proposed that the main hydrodynamic resistance occurs in the nodes. The bubble surfaces are mobile, thus the surface velocity is non-zero, yielding another form for $k(\varepsilon) = K_{\mathrm{n}}L^2\varepsilon^{1/2}$, leading to:

$$\begin{aligned} V_{\mathrm{f}} &= \frac{K_{\mathrm{n}}\rho g L^2}{\mu}\varepsilon^{1/2} = \left(\frac{K_{\mathrm{n}}\rho g L^2}{\mu}\right)\cdot\left(\frac{v_{\mathrm{s}}}{v_{\mathrm{f}}}\right)^{1/2} \\ &= \left(\frac{K_{\mathrm{n}}\rho g L^2}{\mu}\right)^{2/3}\cdot {v_{\mathrm{s}}}^{1/3} = \omega\cdot {v_{\mathrm{s}}}^{1/3} \end{aligned} \tag{3}$$

In this node-dominated regime, K_{n} is a dimensionless number, describing the node permeability. Experimental results could be expressed as $v_{\mathrm{f}} \sim {v_{\mathrm{s}}}^{\alpha}$, where α is the fitting parameter, and simple power-law adjustments of forced drainage provide an exponent α between 1/3 and 1/2.[13,46]

In free drainage, we focused on the time variation of the liquid fraction within a foam at multiple locations, which follows power-laws: $\varepsilon(z) = t^{-\beta}$. The exponent β depends on the parameter $\chi = z/z_0\ (t_0/t)^{1/2}$ ($z = 0$ at the foam top).[16] Here, z_0 and t_0 are the length scales and the typical time defined by $z_0 = C\gamma/2\rho g L$ and $t_0 = C\gamma\mu/2K_{\mathrm{x}}(\rho g)^2L^3$. C is the constant, γ is the surface tension, K_{x} is the dimensionless parameter depending on the drainage regime: K_{c} for rigid surfaces and K_{n} for mobile ones

$$\begin{aligned} &\varepsilon \sim t^{-2/3} \quad \text{for} \quad \chi < 1, \\ &\varepsilon \sim t^{-1} \quad \text{for} \quad \chi > 1(\text{less mobile, PB-dominated}) \end{aligned} \tag{4}$$

$$\begin{aligned} &\varepsilon \sim t^{-1} \quad \text{for} \quad \chi < 1, \\ &\varepsilon \sim t^{-2} \quad \text{for} \quad \chi > 1(\text{mobile, node-dominated}) \end{aligned} \tag{5}$$

In the transition range, the flow is in a single PB with interfaces that are neither perfectly rigid nor perfectly mobile.

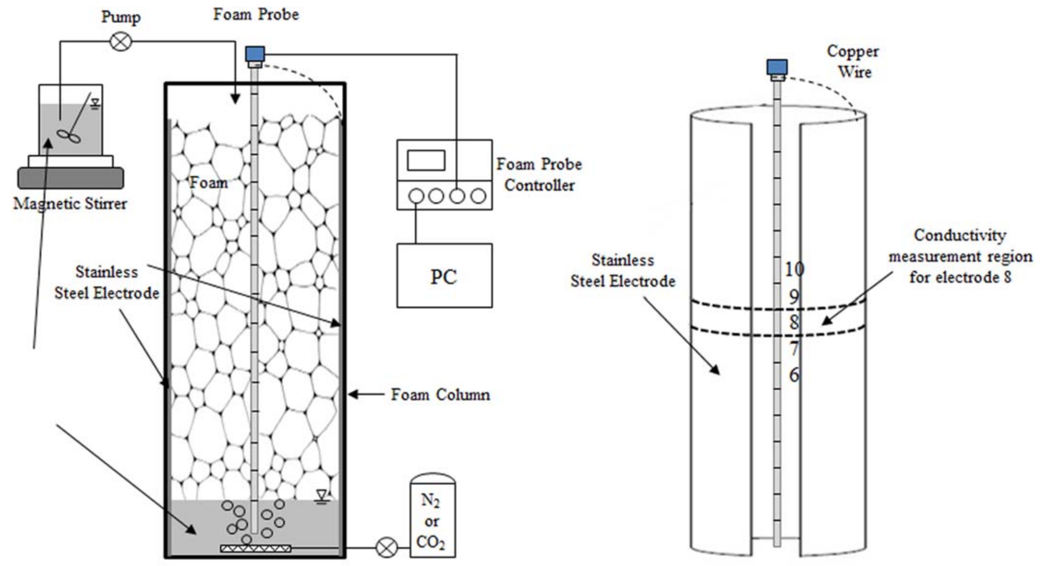

Figure 1. Schematic diagram of the multipoint electrical resistance measurement system for characterization of drainage regimes and stability.

[Color figure can be viewed in the online issue, which is available at wileyonlinelibrary.com.]

Material and Methods

Foaming solutions

SDS of high purity and SDBS were purchased from Sigma-Aldrich (St. Louis, MO) and were used as a foaming agent to represent common anionic surfactants. Our technique was applicable for this kind of nonpolar liquids. In a typical preparation, an aqueous solution was prepared by dissolving powder surfactants in deionized (DI) water, followed by filtration through a 0.22 μm filter (Millipore Corp., Molsheim, France). A typical concentration was 1.2×10^{-2} mol/L (1.5 CMC) for SDS aqueous solutions, which is slightly above the critical micelle concentration (CMC) estimated at the 8.2×10^{-3} mol/L.[47] To compare existing results in the literature, concentrations of SDS were adjusted in the range of 8.2×10^{-3} mol/L (1.0 CMC) to 1.6×10^{-2} mol/L (2.0 CMC). The CMC of SDBS was equal to 1.2×10^{-3} mol/L,[48] and this surfactant was particularly stable. SDBS concentration was 1.8×10^{-3} mol/L (1.5 CMC) for forced drainage and 1.2×10^{-2} mol/L (10 CMC) for free drainage to reduce coarsening effects. All foams were made by injecting nitrogen gas through a sintered air diffuser inside the foaming solution at a controlled gas flow rate of 0.1 m^3/h.

Experimental set-up

All experiments for the study of drainage were performed with the multi-point electrical resistance measurement system (Figure 1). The input of nitrogen gas into the foaming solution produced foams along the height of the test column (diameter of 15.2 cm and height of 1.0 m). This measurement apparatus consisted of a stainless steel electrode placed around the inner edge of the column, a multi-point foam probe placed at the center of the column, and a controller connected to the main body of the foam probe. Foam probe and controller were developed by Charis Technology (Maidstone, Kent, UK) and they allowed for continuous monitoring and recording of total foam heights and electrical resistance. The probe consisted of 16 electrodes at regular intervals (7.5 cm). When a voltage (1.0 V) is applied to the electrodes, the response of electrical currents at each electrode was logged in a PC every seven seconds by the controller. It provided a conductance reading that can be converted to a specific conductivity (σ) by means of the following equation.[41,42,49]

$$\sigma=\lambda \cdot \theta=\frac{\ln(b/a)}{2\pi lR} \tag{6}$$

where λ is the conductance (S), θ is the cell constant, which is equal to the distance between electrodes divided by the cross-sectional area of electrodes, R is the resistance (Ω) ($1/R =$ conductance), and b, a, and l are the diameter of column from probe center to wall (here 15.2 cm), the diameter of the probe (here 1.2 cm), and the length of each electrode (here 7.5 cm), respectively.

Drainage experiments

The protocol for all forced drainage experiments comprised the following steps. First, a foam layer (80 cm) was prepared in the test column and was allowed to drain completely under normal gravity conditions to obtain a relatively uniform column of dry foam (typically liquid fraction $\varepsilon < 10^{-4}$). Once the foam was dry, the same foaming solution was added to the top of the column at a controlled flow rate (Q). As this solution migrated downward through the dry foam, a wet front traveled down the foam column at a steady velocity (v_f). The experiment was terminated when the wet front reached the bottom of the foam resulting in almost uniformly wet foam. Electrical resistance, measured at multiple locations along the foam column, was used to follow the advancing wet front. This front velocity will depend on the injected superficial velocity by the mass conservation. Adding liquid for a time Δt at the top produced uniformly wetted foam behind the front spanning a volume ($v_f \cdot A \cdot \Delta t$) and the liquid fraction (ε) can be calculated as:

$$\varepsilon = \frac{Q \cdot \Delta t}{v_f \cdot A \cdot \Delta t} = \frac{v_s}{v_f} \quad (7)$$

A free drainage experiment of SDBS foams was investigated to validate the result of the drainage regime by the forced drainage experiment and to improve the study of foam stability. In free drainage experiments, the drainage dynamics were observed by the electrical resistance technique which allows to follow the liquid fraction as a function of time, $\varepsilon(t)$, in several points of the foam column. This provided the drainage curves of the liquid fraction in the foam at any time, which can be normalized by the initial liquid fraction obtained after complete foam formation. Together with the drainage curves, we obtained continuous on-line profiles of total height of the foam, $H(t)$, then the foam stability could be characterized by its half-life time, defined as the time required for the foam to be reduced by half.[50]

Results and Discussion

Calibration curves and detection limits

Figure 2 presents the relationship between the relative conductivity and the liquid fraction of anionic surfactant (SDS) foams. The measurement region of the probe is a circular slice through the column and the shape of the regions is maintained by the interaction of the electric field from each electrode with that from neighboring electrodes. Relative conductivity values were computed from electrical resistance measurement data obtained at multiple locations in the foam column. The error bars are the sample standard deviations. The liquid fraction was calculated according to Eq. 7. This calculation was based on average values of the macroscopic drainage rate during the drainage through the foam column at individual injected superficial velocities. The lower detection limit for relative conductivity is 0.0017, corresponding to the liquid fraction of 0.0046. In a two-phase foam system, a similar relationship between the relative conductivity and the liquid fraction has been developed by Lemlich.[43] The following equation is particularly useful, as it requires only a measure of the relative conductivity for predicting the liquid fraction

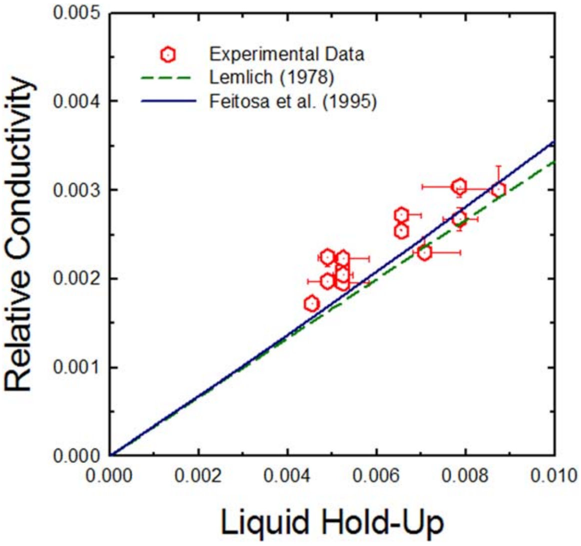

Figure 2. Relationship between the relative conductivity and the liquid fraction for anionic surfactant (SDS) foams.

The liquid hold-up was computed from the macroscopic drainage rate obtained at individual injected superficial velocities during forced drainage experiments. The lower detection limit for relative conductivity is 0.0017, corresponding to the liquid fraction of 0.0046. The dotted lines were fitted to the Eq. 8 and the solid lines were fitted to the Eq. 9. [Color figure can be viewed in the online issue, which is available at wileyonlinelibrary.com.]

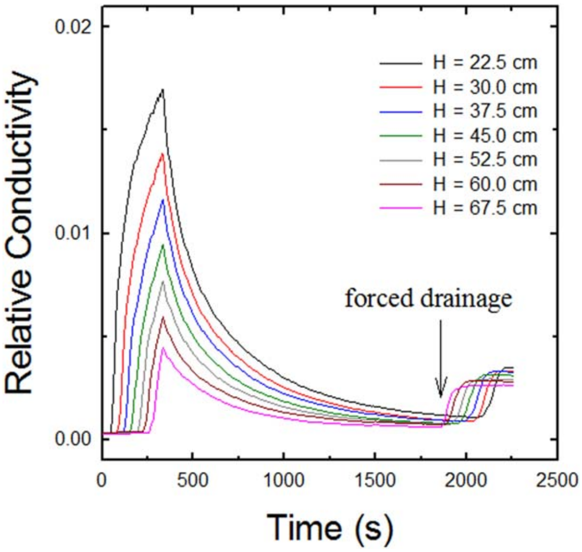

Figure 3. Representative relative conductivity profiles for foam probe electrodes from the bottom ($H = 22.5$ cm) to the top ($H = 67.5$ cm) during foam formation and forced drainage experiments.

[Color figure can be viewed in the online issue, which is available at wileyonlinelibrary.com.]

$$\varepsilon = 3 \cdot \sigma_r = 3 \cdot \frac{\sigma_f}{\sigma_l} \quad (8)$$

where σ_f and σ_l are the specific conductivity in the foam and bulk liquid phase, respectively. For our experimental setup, all parameters in Eq. 6 except λ were constant, and the relative conductance was, therefore, equal to the relative conductivity. The dotted line was fitted to Eq. 8 in Figure 2 to demonstrate the capacity of continuous on-line measurements of the liquid fraction. The equation is only valid at lower values of liquid fraction ($\varepsilon < 0.1$),[42] as the liquid remains largely in the PBs with the derivation of this equation.[43,51] As the liquid fraction increases, the relationship becomes sub-linear due to the increasing importance of nodes.[52] For a wider range of liquid fractions, a simple empirical formula (Eq. 9) gave an excellent description of collected data,[39] as shown by the nearly identical solid lines in Figure 2

$$\varepsilon = \frac{3\sigma_r(1+11\sigma_r)}{(1+25\sigma_r+10\sigma_r^2)} \quad (9)$$

When considering all the data conducted for SDS foams, the relative conductivity tends to be higher for our experimental data than for other two fitted lines. As the liquid fraction increases, particularly above approximately 0.007, there is closer agreement between some scatter in the data and Eq. 8. In free drainage, the variation of the liquid fraction along the foam column was computed from Eq. 9 after the measurements of both the conductivity in the foam phase and the conductivity in the bulk liquid phase.

Macroscopic drainage observation

Electrode pairs located at multiple heights of the foam column measured the relative conductivity profiles with time (Figure 3). As the foam developed, the relative conductivity increased, reaching a maximum when gas input was terminated and the foam started draining. As expected, the relative conductivity was higher for electrodes closer to the bulk liquid surface during the foam formation. It could be visually observed that the relative conductivity varied with height, the foam being wettest at the bottom and driest at the top. The foam was allowed to reach a height of 80 cm before the gas was stopped, and then drained out until equilibrium was eventually reached between gravitational and capillary forces. In order to prepare the dried foam column, liquid drainage was continuously allowed until the relative conductivity had similar values at different heights along the foam column. The drainage rate's relationship to vertical location showed that drainage was fastest at the bottom of the foam column and slowest at the top. This observation can be attributed to the higher hydrostatic head at the top, which leads to more resistance to the liquid flow in the foam phase.

The forced drainage method allows an estimation of accurate liquid fraction of the foam. The relative conductivity profiles were enlarged for the forced drainage time in Figure 3 with the heights of 30.0, 37.5, 45.0, and 52.5 cm of the foam column (Figure 4). Once the added solution (9.37×10^{-4} cm/s) has passed each electrode, the relative conductivity started increasing because the wet front traveled down the foam column, and in the limit of long times, approached an equilibrium state. This liquid fraction distribution becomes more and more uniform as drainage proceeds. The front moving down along the foam column did not spread out, but took the form of a solitary wave. This velocity is thus the same as the surface-averaged liquid velocity behind the wave and could be estimated as $v_f = l/t_i$, where t_i is the average time it takes the midpoint of the wet front to migrate from one electrode to another. This macroscopic front drainage velocity was measured in a series of experiments with different superficial velocities.

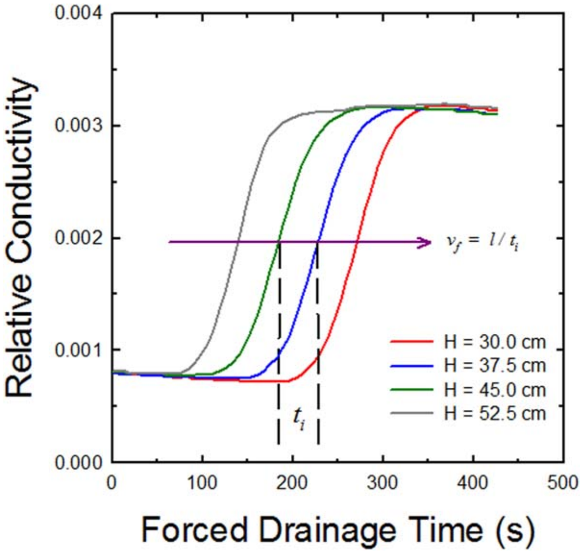

Figure 4. Representative relative conductivity profiles with time during forced drainage experiments.

Average front velocity could be estimated as $v_f = l$ (=7.5 cm)/t_i through a series of drainage experiments with different superficial velocities for aqueous foam stabilized with sodium dodecyl sulfate (SDS) at the concentration of 1.2×10^{-2} mol/L (1.5 CMC). Superficial velocity was 9.37×10^{-4} cm/s. [Color figure can be viewed in the online issue, which is available at wileyonlinelibrary.com.]

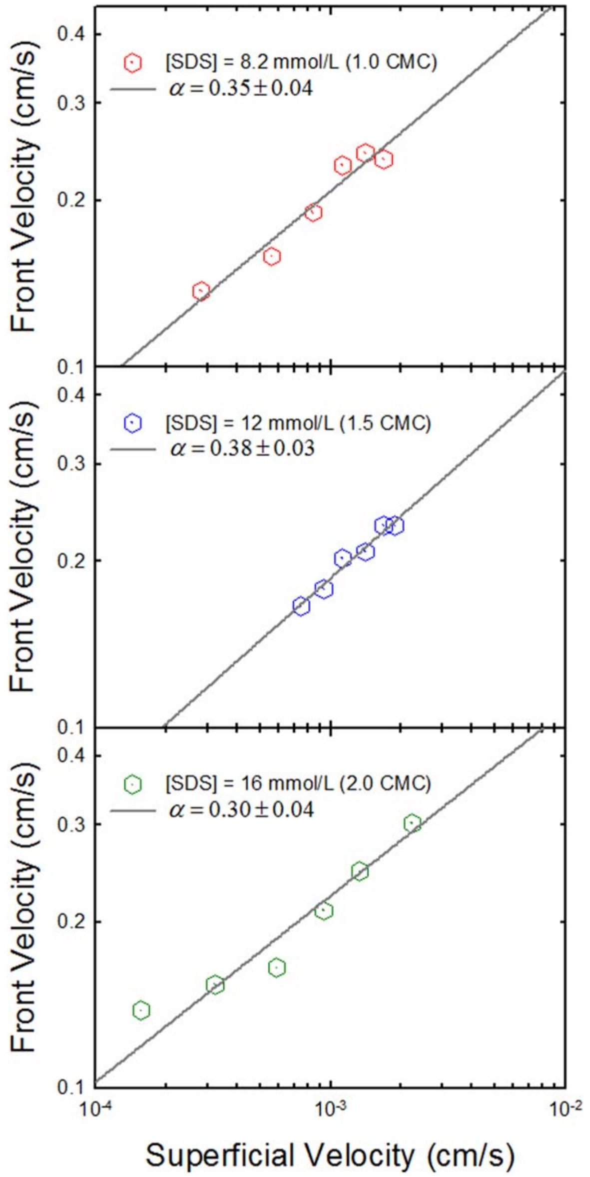

Figure 5. Relationship between the front velocity and the superficial velocity for aqueous foams stabilized with sodium dodecyl sulfate (SDS) at the concentration of 8.2×10^{-3} mol/L (1.0 CMC), 1.2×10^{-2} mol/L (1.5 CMC), and 1.6×10^{-2} mol/L (2.0 CMC), respectively.

Each line indicated power-law relations with an exponent α. [Color figure can be viewed in the online issue, which is available at wileyonlinelibrary.com.]

Method validation

The capacity of the technique was confirmed by the estimation of macroscopic drainage rates through a series of forced drainage experiments for aqueous foam stabilized with SDS. Simple surfactant foams were first tested at a range of injected superficial velocities. The concentrations of SDS solutions

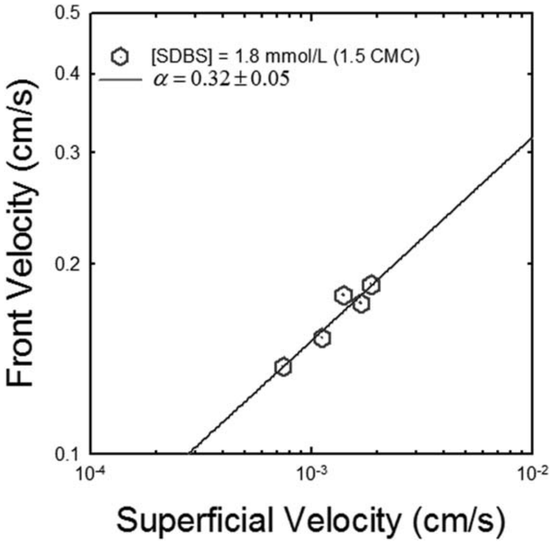

Figure 6. Relationship between the front velocity and the superficial velocity for aqueous foams stabilized with sodium dodecylbenzenesulfonate (SDBS) at the concentration of 1.8 × 10^{-3} mol/L (1.5 CMC).

The line indicated power-law relations with an exponent $\alpha = 0.32 \pm 0.05$. [Color figure can be viewed in the online issue, which is available at wileyonlinelibrary.com.]

used in this experiments were 8.2 × 10^{-3} mol/L (1.0 CMC), 1.2 × 10^{-2} mol/L (1.5 CMC), and 1.6 × 10^{-2} mol/L (2.0 CMC), respectively. These values were selected to compare the performance of the drainage regime with the existing studies using other measurement techniques.

It was reported that a power-law relationship between the front velocity and the superficial velocity was in a good agreement with experimental findings. We found that a simple power-law yielded an exponent $\alpha = 0.35 \pm 0.04$ for 1.0 CMC, $\alpha = 0.38 \pm 0.03$ for 1.5 CMC, and $\alpha = 0.30 \pm 0.04$ for 2.0 CMC, respectively (Figure 5). Power-law relationships were analyzed by regression statistics with confidence level of 95%. *P*-values were less than 0.001 for all relationships. The estimated power laws as a fitting parameter indicated that the bubble surfaces are mobile, i.e., in the node-dominated, since the power-law exponent was close to its theoretical value ($\alpha = 1/3$) in Eq. 3. Under the same foaming conditions, the results obtained by the multiple light scattering technique[13] and the segmented capacitance sensors with two parallel plates[28] were in good agreement with those used. In two-phase foams, the electrical resistance measurement method developed in this work was validated.

Drainage behavior of SDBS foams

Drainage regime of a column of draining aqueous foam stabilized with SDBS was characterized by both forced and free drainage experiments in which local drainage rates are measured by the electrical resistance technique. Forced drainage experiments were carried out for the SDBS foam at the concentration of 1.8 × 10^{-3} mol/L (1.5 CMC). The variation of the front velocity with the superficial velocity of the injected fluid was investigated to determine the drainage regime (Figure 6). The data were fitted with power-laws over a range of almost two orders of magnitude of flow rates. The power-law exponent α (= 0.32 ± 0.05) was close to the theoretical value for the node-dominated regime, where dissipation mainly occurred in the nodes with the mobile PB surfaces (Eq. 3).

Free drainage experiments were performed to verify the drainage properties (i.e., node-dominated regime) obtained from the forced drainage experiment. To validate the result obtained from forced drainage experiments, the same foaming solution was used in free drainage experiments. The evolution of the liquid fraction over time was followed at a fixed position in the foam, 10 cm from the top. The liquid fraction was calculated from the relative conductivity in Eq. 9. The drainage curve could be normalized by the initial liquid fraction in foams ($\varepsilon_0 = 0.002$) obtained after the foam formation. Free drainage curves showed the power-law decay and the time scale on which power-law behavior appears was of the order of 100 s (Figure 7). From the long-time scale, the drainage regime can be determined from the exponent of a power-law, $\varepsilon = t^{-\beta}$ (Eqs. 4 or 5).

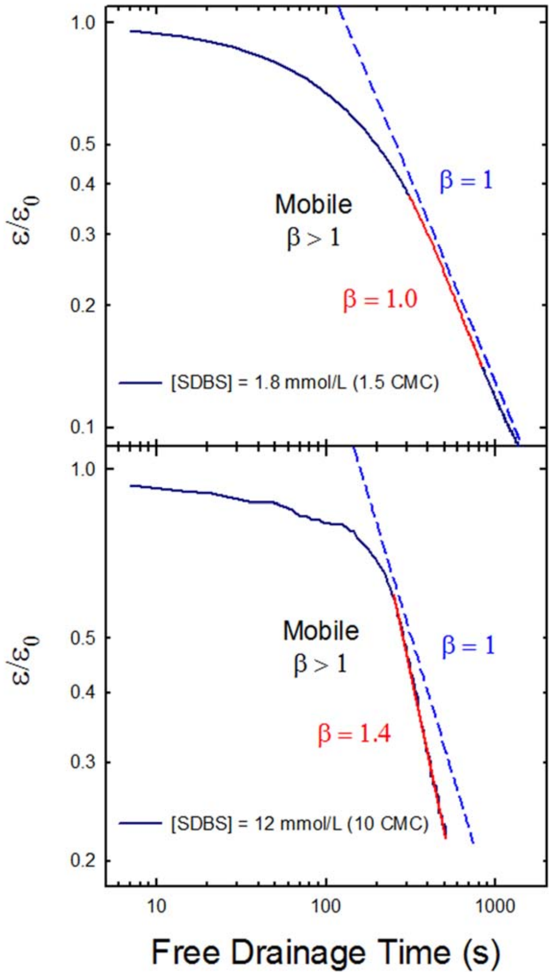

Figure 7. Normalized liquid fractions with free drainage time for aqueous foams stabilized with SDBS at the concentration of 1.8 × 10^{-3} mol/L (1.5 CMC) and 1.2 × 10^{-2} mol/L (10 CMC), respectively.

Drainage curve corresponds to a fixed height, 10 cm below the top of the foam. The initial liquid fraction in foams was 0.002 and the exponent β was estimated to be 1.0 and 1.4, respectively. [Color figure can be viewed in the online issue, which is available at wileyonlinelibrary.com.]

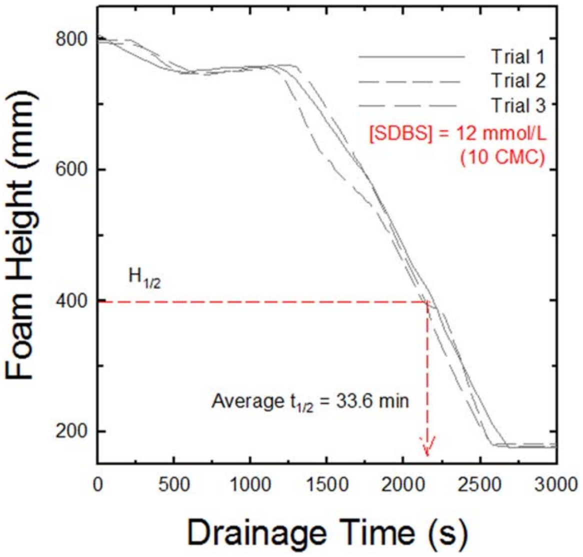

Figure 8. Representative variation of foam height with the corresponding elapsed time during free drainage of SDBS foams.

Foam half-life time ($t_{1/2}$) was estimated when the height reached at half of initial foam height ($H_{1/2}$) and was 33.6 min. [Color figure can be viewed in the online issue, which is available at wileyonlinelibrary.com.]

High concentrations of SDBS ($[\mathrm{SDBS}]/\mathrm{CMC}_{\mathrm{SDBS}} = 10$) were used to strongly minimize the coalescence-induced foam destabilization.[30] At higher concentration, the liquid fraction was dramatically decreased after certain drainage times (Figure 7). This suggests that higher surfactant concentrations cause more stable foam for a long time, however, the drainage regime was not changed with similar theoretical values of power-law exponent. The value of the exponent (β) was estimated to be 1.4 for the SDBS concentration of 10 CMC and supports our expectation of high surface mobility in the PB walls during drainage. These results confirmed the previous experiment's results, showing that the node-dominated regime was found in forced drainage experiments.

Foam stability determination

In the majority of studies where the drainage regime is predicted, no attempt was made to investigate foam stability. The time of rupture of half of the foam column, $t_{1/2}$, was the commonly used to quantify foam stability. The initially produced foam column decayed to half of its height. The foam probe used in this study continuously measured the variation of total foam heights during the foam formation and drainage. The foam heights were plotted versus the corresponding elapsed time for the free drainage of SDBS foams (Figure 8). Typical concentration of SDBS was 1.2×10^{-2} mol/L (10 CMC) and the estimated $t_{1/2}$ was 33.6 min. The capability of this simple automated method to estimate the half-life time could be applied for testing and predicting of foams of extremely varying stability. The technique is relatively low-cost, easy to use, and is therefore useful for the study of foam drainage for both qualitative and quantitative description of various foaming systems. However, important issues must be clarified for a complete understanding of the correlation between the drainage regime and foam stability.

Conclusions

The measurement of foam electrical properties provides a basis for characterizing the foam drainage properties that are not easily determined in various stable foams. A new approach to the characterization of foam drainage properties has been proposed by an improved measurement device based on the electrical resistance of foam. This device provides a continuous on-line measurement of the electrical resistance at multiple locations along the foam column. The experimental approaches include estimations of macroscopic drainage rates through the foam structure, and analysis of the regime for standing foams. The results clearly showed the potential of the multi-point electrical resistance measurement system to yield information on the liquid distribution, drainage rates, foam heights, and stability. Determination of drainage regime for SDS foams was first attempted by this technique, which enables both real-time monitoring and intervention in foam development. In our experiments, all tested SDS foams were likely to exhibit the node-dominated drainage regime. This result was in a good agreement with the findings of existing drainage studies using other measurement techniques in the literature. Our developed method designed to characterize drainage regime was validated for SDS foams.

This research further explored these results using SDBS. Results showed that all tested SDBS foams were also likely to exhibit the node-dominated drainage regime based on both forced and free drainage studies. Experiments suggest that our developed technique was applicable for any other foams stabilized with surfactants to determine drainage regime.

This research also introduced an accurate method for quantifying foam stability that can simultaneously measure variations of foam height with electrical resistance at multiple locations. The data obtained are potentially useful for predicting the evolution of the liquid content and the foam height as a function of time that is typically assessed as foam stability. This inexpensive and efficient method for measuring electrical resistance and liquid variations in real-time may be particularly relevant to monitoring programs for unidentified foams in many industries.

Acknowledgments

This research was partially supported by funding from the San Francisco Public Utilities Commission (SFPUC), a department of the City and County of San Francisco, and Department of Civil and Environmental Engineering at the University of California, Berkeley. The authors thank Steve Gallagher for his technical advice on the multi-point electrical resistance measurement system.

Notation

A = cross-sectional area of the foam column, cm^2
a = radius of foam probe, cm
b = distance from probe center to wall, cm
g = gravitational acceleration, m/s^2
H = foam height, cm
k = permeability, m^2
K_c = dimensionless PB-dominated permeability number
K_n = dimensionless node-dominated permeability number
L = length of PB, m
l = length of electrode on foam probe, cm
Q = controlled flow rate, m^3/h
R = resistance, Ω
t = time, s
t_i = drainage time during forced drainage experiment, s

$t_{1/2}$ = foam half-life time, s
v_f = front drainage velocity, cm/s
v_s = superficial velocity, cm/s
z = vertical coordinate, cm

Greek letters

α = power-law exponent in forced drainage experiment
β = power-law exponent in free drainage experiment
ε = liquid fraction
θ = cell constant in Eq. 6
λ = electrical conductance, S
μ = bulk viscosity of foaming solution, Pa · s
ρ = density, kg/m^3
σ = specific conductivity, S/cm

Literature Cited

1. Dean RB. The formation of bubbles. *J Appl Phys.* 1944;15(5):446–451.
2. Bikerman JJ. *Foams*. Berlin: Springer-Verlag, 1973.
3. Exerowa D, Kruglyakov PM. *Foams and Foam Films: Theory, Experiment, Application*. Amsterdam: Elsevier, 1998.
4. Hutzler S, Weaire D, Crawford R. Convective instability in foam drainage. *Europhys Lett.* 1998;41(4):461–465.
5. Vardar-Sukan F. Foaming: consequences, prevention and destruction. *Biotechnol Adv.* 1998;16(5–6):913–948.
6. Soddell JA, Seviour RJ. Microbiology of foaming in activated sludge plants. *J Appl Bacteriol.* 1990;69(2):145–176.
7. Pujol R, Duchene P, Schetrite S, Canler JP. Biological foams in activated sludge plants: characterization and situation. *Water Res.* 1991; 25(11):1399–1404.
8. Frigon D, Guthrie RM, Bachman GT, Royer J, Bailey B, Raskin L. Long-term analysis of a full-scale activated sludge wastewater treatment system exhibiting seasonal biological foaming. *Water Res.* 2006;40(5):990–1008.
9. Petrovski S, Dyson ZA, Quill ES, McIlroy SJ, Tillett D, Seviour RJ. An examination of the mechanisms for stable foam formation in activated sludge systems. *Water Res.* 2011;45(5):2146–2154.
10. Weaire D, Hutzler S, Verbist G, Peters E. A review of foam drainage. *Adv Chem Phys.* 1997;102:315–374.
11. Saint-Jalmes A, Langevin D. Time evolution of aqueous foams: drainage and coarsening. *J Phys: Condens Matter* 2002;14(40):9397–9412.
12. Stevenson P. On the forced drainage of foam. *Colloid Surf A* 2007; 305(1–3):1–9.
13. Saint-Jalmes A, Zhang Y, Langevin D. Quantitative description of foam drainage: transitions with surface mobility. *Eur Phys J E Soft Matter* 2004;15(1):53–60.
14. Safouane M, Saint-Jalmes A, Bergeron V, Langevin D. Viscosity effects in foam drainage: Newtonian and non-Newtonian foaming fluids. *Eur Phys J E Soft Matter* 2006;19(2):195–202.
15. Verbist G, Weaire D, Kraynik AM. The foam drainage equation. *J Phys: Condens Matter* 1996;8(21):3715–3731.
16. Koehler SA, Hilgenfeldt S, Stone HA. A generalized view of foam drainage: experiment and theory. *Langmuir* 2000;16(15):6327–6341.
17. Neethling SJ, Lee HT, Cilliers JJ. A foam drainage equation generalized for all liquid contents. *J Phys: Condens Matter* 2002;14(3):331–342.
18. Saint-Jalmes A. Physical chemistry in foam drainage and coarsening. *Soft Matter* 2006;2(10):836–849.
19. Lorenceau E, Louvet N, Rouyer F, Pitois O. Permeability of aqueous foams. *Eur Phys J E Soft Matter* 2009;28(3):293–304.
20. Kruglyakov PM, Karakashev SI, Nguyen AV, Vilkova NG. Foam drainage. *Curr Opin Colloid Interface Sci.* 2008;13(3):163–170.
21. Biance A-L, Delbos A, Pitois O. How topological rearrangements and liquid fraction control liquid foam stability. *Phys Rev Lett.* 2011;106(6):068301.
22. Leonard RA, Lemlich R. A study of interstitial liquid flow in foam: I. Theoretical model and application to foam fractionation. *AIChE J.* 1965;11(1):18–25.
23. Weaire D, Pittet N, Hutzler S, Pardal D. Steady state drainage of an aqueous foam. *Phys Rev Lett.* 1993;71(16):2670–2673.
24. Neethling SJ, Lee HT, Grassia P. The growth, drainage and breakdown of foams. *Colloid Surf A.* 2005;263(1–3):184–196.
25. Saint-Jalmes A, Vera MU, Durian DJ. Free drainage of aqueous foams: Container shape effects on capillarity and vertical gradients. *Europhys Lett.* 2000;50(5):695–701.
26. Carey E, Stubenrauch C. Free drainage of aqueous foams stabilized by mixtures of a non-ionic (C12DMPO) and an ionic (C(12)TAB) surfactant. *Colloid Surf A.* 2013;419:7–14.
27. Cervantes-Martínez A, Saint-Jalmes A, Maldonado A, Langevin D. Effect of cosurfactant on the free-drainage regime of aqueous foams. *J Colloid Interface Sci.* 2005;292(2):544–547.
28. Durand M, Martinoty G, Langevin D. Liquid flow through aqueous foams: From the Plateau border-dominated regime to the node-dominated regime. *Phys Rev E.* 1999;60(6):R6307–R6308.
29. Koehler SA, Hilgenfeldt S, Stone HA. Liquid flow through aqueous foams: The node-dominated foam drainage equation. *Phys Rev Lett.* 1999;82(21):4232–4235.
30. Carn F, Colin A, Pitois O, Vignes-Adler M, Backov R. Foam drainage in the presence of nanoparticle surfactant mixtures. *Langmuir* 2009;25(14):7847–7856.
31. Barigou M, Deshpande NS, Wiggers FN. An enhanced electrical resistance technique for foam drainage measurement. *Colloid Surf A* 2001;189(1–3):237–246.
32. Vera MU, Saint-Jalmes A, Durian DJ. Scattering optics of foam. *Appl Opt.* 2001;40(24):4210–4214.
33. Hutzler S, Verbist G, Weaire D, Vandersteen JA. Measurement of foam density profiles using AC capacitance. *Europhys Lett.* 1995; 31(8):497–502.
34. Chang KS, Lemlich R. Study of the electrical conductivity of foam. *J Colloid Interface Sci.* 1980;73(1):224–232.
35. Datye AK, Lemlich R. Liquid distribution and electrical conductivity in foam. *Int J Multiphase Flow* 1983;9(6):627–636.
36. Weaire D, Findlay S, Verbist G. Measurement of foam drainage using AC conductivity. *J Phys: Condens Matter.* 1995;7(16):L217–L222.
37. Wilde PJ. Foam measurement by the microconductivity technique: an assessment of its sensitivity to interfacial and environmental factors. *J Colloid Interface Sci.* 1996;178(2):733–739.
38. Phianmongkhol A, Varley J. A multi point conductivity measurement system for characterisation of protein foams. *Colloid Surf B.* 1999;12(3–6):247–259.
39. Feitosa K, Marze S, Saint-Jalmes A, Durian DJ. Electrical conductivity of dispersions: from dry foams to dilute suspensions. *J Phys: Condens Matter.* 2005;17(41):6301–6305.
40. Brown AK, Isbell C, Gallagher S, Dodd PW, Varley J. An improved method for controlling foams produced within bioreactors. *Food Bioprod Process.* 2001;79(C2):114–121.
41. Varley J, Boyd JWR, Gallagher S, Brown AK, Dodd PW. Correlation between conductivity and liquid hold-up for a multi-segment industrial foam probe for fermentation. *Biochem Eng J.* 2004;19(3):199–210.
42. Varley J, Brown AK, Boyd JWR, Dodd PW, Gallagher S. Dynamic multi-point measurement of foam behaviour for a continuous fermentation over a range of key process variables. *Biochem Eng J.* 2004;20(1):61–72.
43. Lemlich R. Theory for limiting conductivity of polyhedral foam at low density. *J Colloid Interface Sci.* 1978;64(1):107–110.
44. Mcevoy J, Giger W. Determination of linear alkylbenzenesulfonates in sewage sludge by high-resolution gas chromatography/mass spectrometry. *Environ Sci Technol.* 1986;20(4):376–383.
45. Feijtel T, Vits H, Murray-Smith R, van Wijk R, Koch V, Schröder R, Berge WT. Fate of LAS in activated sludge wastewater treatment plants: a model verification study. *Chemosphere* 1996;32(7):1413–1426.
46. Stone HA, Koehler SA, Hilgenfeldt S, Durand M. Perspectives on foam drainage and the influence of interfacial rheology. *J Phys: Condens Matter* 2003;15(1):S283–S290.
47. Bergeron V, Radke CJ. Equilibrium measurements of oscillatory disjoining pressures in aqueous foam films. *Langmuir* 1992;8(12):3020–3026.
48. Carrier V, Colin A. Anisotropy of draining foams. *Langmuir* 2002; 18(20):7564–7570.
49. Zahn M. Electromagnetic Field Theory: A Problem Solving Approach. London: Wiley, 1979.
50. Iglesias E, Anderez J, Forgiarini A, Salager JL. A new method to estimate the stability of short-life foams. *Colloid Surf A* 1995;98(1–2):167–174.
51. Phelan R, Weaire D, Peters EAJF, Verbist G. The conductivity of a foam. *J Phys: Condens Matter* 1996;8(34):L475–L482.
52. Britan A, Liverts M, Ben-Dor G, Koehler SA, Bennani N. The effect of fine particles on the drainage and coarsening of foam. *Colloid Surf A* 2009;344(1–3):15–23.

Manuscript received Sept. 26, 2013; and revision received Apr. 1, 2014.